

SPIO-Annexin V, a potential probe for MRI detection of radiation induced apoptosis

Gh. Haeri¹, H. Rajabi^{1*}, Sh. Akhlaghpour²

¹Department of Medical Physics, Faculty of Medical Sciences, Tarbiat Modares University, Tehran, Iran

²Department of Radiology, Sina Hospital, Tehran University of Medical Science, Tehran, Iran

ABSTRACT

Background: Finding a suitable method for rapid, accurate and reliable estimation of absorbed dose has high priority in management of the radiation exposed persons. Shortly after radiation exposure, apoptosis is a major detriment in proliferative tissues such as the hematopoietic system. Therefore, quantification of apoptosis in these tissues could be useful for rapid estimation of radiation exposure. Annexin V (ANX) is considered as a biological probe for detection of apoptotic cells. The aim of the present study is to investigate the potential suitability of apoptosis quantification for estimation of radiation exposure. **Materials and Methods:** In order to determine the biological distribution of ANX within the mice body after radiation exposure, mice whole body irradiated with 2, 4, 6 and 8 Gy (⁶⁰Co gamma rays). Ten hours later, ANX conjugated with super paramagnetic iron oxide nanoparticles (SPIO-ANX) was administered intravenously and magnetic resonance imaging was conducted 3 hours later. **Results:** Average signal intensities in the regions of interest (ROIs) of the femur bone marrow, liver and testis were calculated and normalized to parafemoral muscle signals. SPIO-ANX accumulated in bone marrow of irradiated groups and significantly decreased the normalized mean of signal intensity for bone marrow in comparison with control group ($p < 0.01$). **Conclusion:** Tracing and quantification of SPIO-ANX in bone marrow can be used as an indicator for radiation exposure. However, development and optimization of the assay are necessary for discrimination between different radiation doses.

Keywords: Apoptosis, radiation exposure, magnetic resonance imaging, dose estimation, annexin V.

► Original article

*** Corresponding author:**

Dr. Hossein Rajabi,

Fax: +98 21 88006544

E-mail: hRajabi@modares.ac.ir

Received: April 2013

Accepted: Aug. 2013

Int. J. Radiat. Res., July 2014;
12(3): 217-222

INTRODUCTION

Rapid, accurate and reliable estimation of absorbed dose has great importance in triage and clinical management of the radiation exposed individuals⁽¹⁾. Dose assessments based on current cytogenetic assays are limited with many drawbacks because cytogenetic assays typically require few days to produce acceptable results that may be vital for treatment of victims⁽²⁻⁴⁾ so, developing the methods for fast biodosimetry have great importance.

Shortly after radiation exposure, apoptosis is a major detriment in proliferative tissues such as the hematopoietic system⁽⁵⁾. Therefore, quantification of apoptosis in these tissues could be useful for rapid estimation of radiation exposure. There are several methods for detection of apoptotic cells⁽⁶⁾. During the early stage of apoptosis, Phosphatidylserine that is binned to the inner leaflet of the lipid bilayer in normal cells is translocated to the external surface of the cells⁽⁷⁾. Annexin V (ANX) is a member of the family of calcium and phospholipid binding proteins with high specific

affinity for Phosphatidylserine. ANX is considered as a biological probe for detection of apoptotic cells (8). ANX could potentially deliver carried materials to sites containing apoptotic cells. ANX had been labeled with different fluoresceins (8-10), radionuclides (11-14) and magnetic particles (15, 16) for detection and measurement of apoptosis.

In order to use magnetic resonance imaging (MRI) as a noninvasive technique for detection of apoptosis, ANX can be conjugated with superparamagnetic materials (17). The advantages of MRI are high spatial resolution, excellent contrast and ability to simultaneously demonstrate the anatomy, physiology and molecular events (18).

In the present study, we have administered ANX conjugated with superparamagnetic iron oxide nanoparticles (SPIO-ANX) to irradiated mice. Animals were imaged to determine the biological distribution of SPIO-ANX within the mice body after irradiation. The objective of this study is developing a noninvasive imaging method as a new modality for fast dose estimation.

MATERIALS AND METHODS

Chemicals

SPIO was purchased from Micromod Company (Germany). It was consisting of an iron oxide core (size of single iron oxide grain about 50 nm) coated with dextran. The concentration of iron in Micromod SPIO was 2.4 mg per ml. SPIO-ANX was obtained from Miltenyi Biotec (Gladbach, Germany). It was consisting of an iron oxide core (size of single iron oxide grain about 10–12 nm) coated with dextran, conjugated to ANX protein. The concentration of iron and ANX in Miltenyi SPIO-ANX were 0.054 mg and 30 µg per ml respectively (16).

Animals

Ten-week-old Swiss male albino mice were purchased from the Pasteur Institute (Tehran-Iran). They were housed in the university animal house with good conditions and given standard mouse pellet and water ad libitum. All

animals were kept under controlled lighting conditions (light: dark, 12:12 hours) and temperature (23 ± 2 °C). All the animal experiments followed a protocol approved by the Institutional Animal Care and Use Committee of the Iranian Institute of Radiological and Medical Sciences. Animals were randomly divided into 9 groups (1-9) of 5 mice in each group:

Group1: Mouse received Saline by intravenous (iv) injection (Control)

Group2: Mouse received 100 µL SPIO (iv)

Group3: Mouse received 100 µL SPIO-ANX (iv)

Group4: Mouse received Single 8 Gy gamma radiation dose + Saline (iv) (Radiation control)

Group5: Mouse received single 8 Gy gamma radiation dose + 100 µL SPIO (iv)

Group6: Mouse received single 2 Gy irradiation + 100 µL SPIO-ANX (iv)

Group7: Mouse received single 4 Gy irradiation + 100 µL SPIO-ANX (iv)

Group8: Mouse received single 6 Gy irradiation + 100 µL SPIO-ANX (iv)

Group9: Mouse received single 8 Gy irradiation + 100 µL SPIO-ANX (iv)

Irradiation

Mice were placed in a ventilated Plexiglas cage and irradiated (whole body) with gamma rays using a ⁶⁰Co radiotherapy unit (Theratron, 780C, Canada) at the dose rate of 50 cGray/min, SSD=80 cm (Source- Subject Distance) and temperature 23 ± 2 °C. The non-irradiated control mice were treated exactly the same way, except the ⁶⁰Co source rod was not raised the shielding (not irradiated). After irradiation, mice have been returned to animal house.

Magnetic resonance imaging

Ten hours after irradiation, 100 µL of imaging agent (SPIO or SPIO-ANX) was administrated iv to the mice groups 5-9. The mice in control and irradiation control groups (groups 1& 3) were treated with normal saline only. Three hours after injection of imaging agent, magnetic resonance imaging was conducted.

Before imaging, mice were anesthetized by intraperitoneal injection of ketamine (20mg/kg) and xylazine (1mg/kg) cocktail. Mice were placed in supine position inside a wrist coil

scanner (to minimize breathing artifacts) and imaging was carried out using a 1.5 Tesla clinical MRI scanner (Philips, Bruker, Etlingen, Germany). We used the coil and imaging protocol of wrist, T2*-weighted gradient echo sequence (TR: 450 ms; TE: 11.5 ms; flip angle: 30°, number of excitations: 1; total acquisition time: 5 min). The field of view was 120×120 mm, image matrix size was 256×256 and slice thickness was 3 mm.

Data analysis

MRI images were analyzed using eFilm software (Version 2.2.1, Merge Healthcare, Milwaukee, USA). Regions of interest (ROIs) were placed in the bone marrow femur, liver, testis and parafemoral muscle. Average signal intensities in the ROIs were calculated and were divided to parafemoral muscle signal for normalization. Analysis of variance was used to determine significant differences among the groups and Mann-Whitney U test to investigate the significance of difference between the groups. Analyzes were performed at significance level of 0.05 using SPSS package (version 13.0).

RESULTS

Normalized mean signal intensity derived from ROIs drawn over MRI images of bone marrow, liver and testis for different

experimental groups are presented in table 1 and figures 2-4. The results are provided as mean ± SD.

Comparison of normalized signal intensity for bone marrow, liver and testis in control and radiation control groups showed that radiation alone did not change the mean signal intensity. In all injected groups, SPIO and SPIO-ANX were mainly accumulated in liver and significantly decreased the mean signal intensity of liver as compared with non injected control mice ($p < 0.01$) (figure 3). In radiation + SPIO-ANX groups, the mean signal intensity of bone marrow significantly decreased in comparison with control and radiation control groups ($p < 0.01$) (figures 1 and 2). However, discrimination of radiation doses from signal intensity of femoral bone marrow couldn't extract statistically ($p > 0.05$). The mean signal intensity of testis did not show significant changes between SPIO-ANX injected groups ($p > 0.05$) (figure 4). Administration of SPIO to irradiated mice showed no SPIO accumulation in bone marrow and there was no significant change in signal intensity of bone marrow as compared with control and radiation control groups ($p > 0.05$).

Administration of SPIO to non irradiated and irradiated mice showed a significant accumulation in testis of both groups but there was no significant difference between them ($p > 0.05$) (figure 4).

Table 1. Normalized signals of tissues in MRI images after whole body irradiation of mice with different doses of gamma radiation and iv injection of imaging agent.

Mice group	Dose (Gy)	Imaging agent	Normalized signal intensity (mean ± S.D.)		
			Bone Marrow	Liver	Testis
1	0	Saline	0.56 ± 0.11	0.8 ± 0.08	1.38 ± 0.13
2	0	SPIO	0.56 ± 0.07	0.26 ± 0.04	0.97 ± 0.17
3	0	SPIO-ANX	0.53 ± 0.05	0.28 ± 0.08	1.17 ± 0.20
4	8	Saline	0.55 ± 0.10	0.78 ± 0.06	1.40 ± 0.11
5	8	SPIO	0.55 ± 0.08	0.25 ± 0.05	0.96 ± 0.13
6	2	SPIO-ANX	0.36 ± 0.08	0.28 ± 0.06	1.23 ± 0.18
7	4	SPIO-ANX	0.32 ± 0.08	0.28 ± 0.07	1.20 ± 0.15
8	6	SPIO-ANX	0.30 ± 0.06	0.26 ± 0.04	1.25 ± 0.14
9	8	SPIO-ANX	0.25 ± 0.06	0.25 ± 0.08	1.15 ± 0.19



Figure 1. Accumulation of SPIO- ANX in femoral bone marrow of gamma irradiated mouse 3 hours after iv injection of SPIO-ANX (arrows).

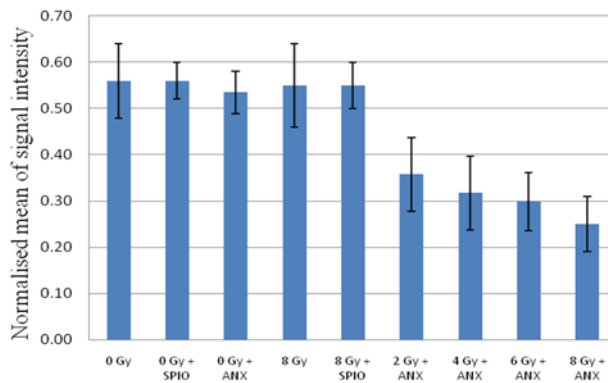


Figure 2. Normalized signals of bone marrow in MRI images after whole body irradiation of mice with different doses of gamma radiation and 3 hours after iv injection of imaging agent (Mean ± SD).

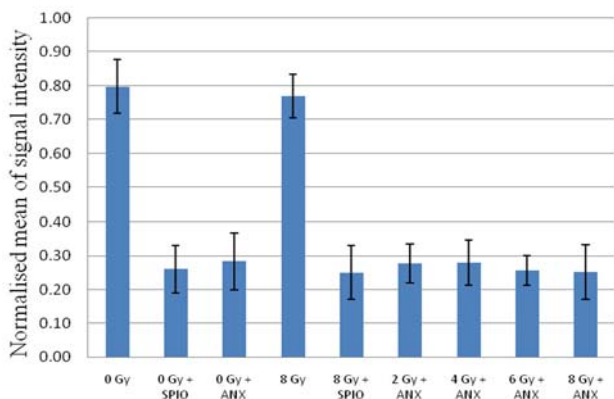


Figure 3. Normalized signals of liver in MRI images after whole body irradiation of mice with different doses of gamma radiation and 3 hours after iv injection of imaging agent (Mean ± SD).

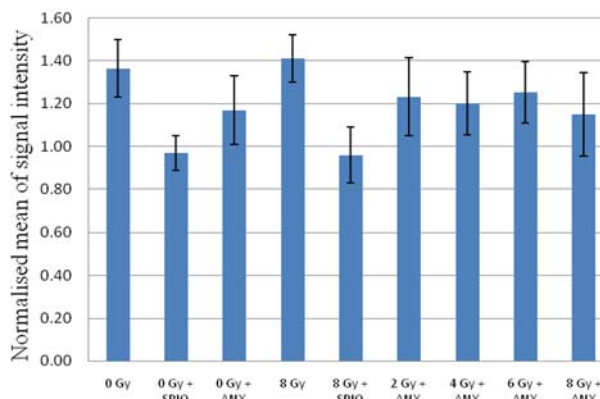


Figure 4. Normalized signals of testis in MRI images after whole body irradiation of mice with different doses of gamma radiation and 3 hours after iv injection of imaging agent (Mean ± SD).

DISCUSSION

Development of improved methods for determining of radiation dose has been identified as a high priority need for emergency triage and clinical management of exposed individuals (19). As MRI scanners are now available in many general hospitals, finding a suitable tracer for noninvasive biodosimetry using MRI imaging could be a useful strategy in radiation accidents and mass casualties. Shortly after exposure to ionizing radiation, considerable apoptosis is induced in proliferative and radiosensitive tissues (20) so tracing and quantifying the induced apoptosis may be suitable for rapid and noninvasive

estimation of radiation absorbed dose. It was identified that most radiation responsive genes which are suitable for dose level discrimination are functionally linked to apoptosis (21).

Tracing of apoptotic cells by radioactive labeled annexin V have been used in different studies (13, 22-24) and it was proposed that apoptosis can be quantified using radiolabel annexin V (14). However, low spatial resolution of scintillation camera and extra exposure of patients to ionizing radiation are the major disadvantages (25).

SPIO have been widely studied for biologic and biomedical applications due to their useful magnetic properties (26). SPIO, or more generally iron-based contrast agents, are very

sensitive to MRI detection in T2 or T2*-weighted images (27). Conjugation of ANX to SPIO creates a targeted MRI contrast agent in which apoptotic cells can be detected through negative contrast in T2-weighted spin echo images (15-17). Miltenyi SPIO-ANX is a ready to use annexin V conjugated with iron microbeads. Miltenyi SPIO are reported to contain single 10–12 nm iron oxide grains (28) and based on diameters of iron grains and average densities of Fe₃O₄ and Fe₂O₃, the numbers of iron in stocks have estimated 4*10¹³ particles/ml (16).

MR spatial resolutions are typically 10–100 micrometers, as compared to Positron Emission Tomography (PET) and Single Photon Emission Tomography (SPECT) resolutions of 1–2 mm (29). Furthermore MRI gives, at the same time, high resolution anatomical information and hence better localization of the apoptotic region. While with PET and SPECT, tissue localization requires fusion of MRI or CT scan images. Thus, biologically targeted super paramagnetic contrast agents can contribute to noninvasive evaluation of irradiated tissues by simultaneously extracting morphological and biochemical data from them.

In this study, testis, bone marrow and liver have been selected for determining biodistribution of SPIO without ANX (as a control group (15) and SPIO-ANX in irradiated mice body. It has been shown that in proliferative tissues, apoptosis occurs shortly after radiation (30), thus time of 10 hours after irradiation has selected for injection of the imaging agents.

An important factor that affects the results is the time of imaging after injection of tracer. We acquired the images 3 hours after injection; however, it has been showed that contrast enhancement appears as early as 30 min after injection of SPIO-ANX (16). In the current study, the signal intensities from target tissues were normalized internally to the average signals from muscle tissues. This likely makes the results independent of the time-gap between injection and imaging. This also rectifies the need for phantom study or any types of external normalization.

One of the major drawbacks for quantification of apoptosis after irradiation is the transient nature of this phenomenon. In highly proliferated normal tissues such as bone marrow, maximum of apoptosis occurs in few hours after radiation and rapidly decreases with passing time (30). Labeling of SPIO-ANX with ^{99m}Tc and analysis of its biodistribution represent the decrease of bone marrow accumulation 24 hours after radiation (data not shown). The information on biodistribution of SPIO-ANX according to the time after irradiation would be helpful to consider its potential as a new modality for biodosimetry and administration of imaging agent in different times after irradiation should be tested for optimization of assay.

Most of the SPIO-ANX metabolically accumulates in the reticuloendothelial system (spleen and liver) (22) which decrease the intensity of signals in liver and spleen (figure 3).

SPIO significantly accumulated in testis of control and irradiated mice but we did not see any accumulation of SPIO-ANX in testis tissue. This is probably due to the large hydrodynamic size (90 nm) of SPIO-ANX nanoparticles to pass through the blood barrier of the testis tissue (table 1, figure 4).

SPIO-ANX was apparently well-tolerated by all mice and none of them exhibited detectable symptoms of systemic toxicity attributable to SPIO.

This is a first report for quantification of apoptosis using MRI in order to estimate the absorbed dose in irradiated tissues. Tracing and quantification of SPIO-ANX in bone marrow can be used as a potential indicator of radiation exposure. However, development and optimization of the assay is necessary for discrimination between different radiation doses.

In summary, SPIO-ANX appears to be a useful in-vivo molecular MRI probe to detect early apoptosis induced by ionizing radiation. Quantification of apoptosis in proliferative tissues shortly after radiation has potential for estimation of absorbed dose and might yield valuable insight into new biodosimetry modality.

ACKNOWLEDGEMENT

This work was supported by a grant from Tarbiat Modares University. The authors have declared that there is no conflict of interest.

REFERENCES

1. Romm H, Wilkins RC, Coleman CN (2011) Biological dosimetry by the triage dicentric chromosome assay: potential implications for treatment of acute radiation syndrome in radiological mass casualties. *Radiat Res*, **175**: 397-404.
2. Prasanna PG, Moroni M, Pellmar TC (2010) Triage dose assessment for partial-body exposure: dicentric analysis. *Health Phys*, **98**: 244-51.
3. Prasanna PG, Hamel CJ, Escalada ND, Duffy KL, Blakely WF (2002) Biological dosimetry using human interphase peripheral blood lymphocytes. *Mil Med*, **167**: 10-2.
4. Ainsbury EA, Bakhanova E, Barquinero JF (2011) Review of retrospective dosimetry techniques for external ionising radiation exposures. *Radiat Prot Dosimetry*, **147**: 573-92.
5. Story MD, Voehringer DW, Malone CG, Hobbs ML, Meyn RE (1994) Radiation-induced apoptosis in sensitive and resistant cells isolated from a mouse lymphoma. *Int J Radiat Biol*, **66**: 659-68.
6. Strauss W, Blankenberg F, Vanderheyden J, Tait J (2008) Translational Imaging: Imaging of Apoptosis. *Handbook of Experimental Pharmacology*: Springer-Verlag Berlin Heidelberg.
7. Gerke V and Moss SE (2002) Annexins: from structure to function. *Physiol Rev*, **82**: 331-71.
8. Vermes I, Haanen C, Steffens-Nakken H, Reutelingsperger C (1995) A novel assay for apoptosis. Flow cytometric detection of phosphatidylserine expression on early apoptotic cells using fluorescein labelled Annexin V. *J Immunol Methods*, **184**: 39-51.
9. Zhang R, Lu W, Wen X (2011) Annexin A5-conjugated polymeric micelles for dual SPECT and optical detection of apoptosis. *J Nucl Med*, **52**: 958-64.
10. Yang SK, Attipoe S, Klausner AP (2006) *In-vivo* detection of apoptotic cells in the testis using fluorescence labeled annexin V in a mouse model of testicular torsion. *J Urol*, **176**: 830-5.
11. Lin KJ, Wu CC, Pan YH (2012) *In-vivo* imaging of radiation-induced tissue apoptosis by (99m)Tc(I)-his (6)-annexin A5. *Ann Nucl Med*, **26**: 272-80.
12. Khoda ME, Utsunomiya K, Ha-Kawa S, Kanno S, Kono Y and Sawada S (2012) An Investigation of the Early Detection of Radiation Induced Apoptosis by 99mTc-Annexin V and 201Thallium-Chloride in a Lung Cancer Cell Line. *J Radiat Res*, **53**: 361-7.
13. Luo QY, Wang F, Zhang ZY (2008) Preparation and bioevaluation of (99m)Tc-HYNIC-annexin B1 as a novel radioligand for apoptosis imaging. *Apoptosis*, **13**: 600-8.
14. Kurihara H, Yang DJ, Cristofanilli M (2008) Imaging and dosimetry of 99mTc EC annexin V: preliminary clinical study targeting apoptosis in breast tumors. *Appl Radiat Isot*, **66**: 1175-82.
15. Dash R, Chung J, Chan T (2011) A molecular MRI probe to detect treatment of cardiac apoptosis *in-vivo*. *Magn Reson Med*, **66**: 1152-62.
16. Smith BR, Heverhagen J, Knopp M (2007) Localization to atherosclerotic plaque and biodistribution of biochemically derivatized superparamagnetic iron oxide nanoparticles (SPIONs) contrast particles for magnetic resonance imaging (MRI). *Biomed Microdevices*, **9**: 719-27.
17. Kettunen M and Brindle K (2005) Apoptosis detection using magnetic resonance imaging and spectroscopy *progress in nuclear resonance spectroscopy*, **47**: 175-85.
18. Sosnovik DE, Nahrendorf M, Weissleder R (2008) Magnetic nanoparticles for MR imaging: agents, techniques and cardiovascular applications. *Basic Res Cardiol*, **103**: 122-30.
19. Pellmar TC and Rockwell S (2005) Priority list of research areas for radiological nuclear threat countermeasures. *Radiat Res*, **163**: 115-23.
20. Kim J, Lee S, Jeon B, Jang W, Moon C, Kim S (2011) Protection of spermatogenesis against gamma ray-induced damage by granulocyte colony-stimulating factor in mice. *Andrologia*, **43**: 87-93.
21. Boldt S, Knops K, Kriehuber R, Wolkenhauer O (2012) A frequency-based gene selection method to identify robust biomarkers for radiation dose prediction. *Int J Radiat Biol*, **88**: 267-76.
22. Yang DJ and Azhdarinia A, Wu P (2001) *In-vivo* and *in-vitro* measurement of apoptosis in breast cancer cells using 99mTc-EC-annexin V. *Cancer Biother Radiopharm*, **16**: 73-83.
23. Lorberboym M, Feldbrin Z, Hendel D, Blankenberg FG, Schachter P (2009) The use of 99mTc-recombinant human annexin V imaging for differential diagnosis of aseptic loosening and low-grade infection in hip and knee prostheses. *J Nucl Med*, **50**: 534-7.
24. Guo MF, Zhao Y, Tian R (2009) *In-vivo* 99mTc-HYNIC-annexin V imaging of early tumor apoptosis in mice after single dose irradiation. *J Exp Clin Cancer Res*, **28**: 136.
25. Andersen LB and Frayne R (2009) Applications of Molecular Imaging with MR. In: Hallgrímsson CWSaB, editor. *Advanced Imaging in Biology and Medicine*: Springer-Verlag Berlin Heidelberg.
26. Lee H, Lee E, Kim do K, Jang NK, Jeong YY, Jon S (2006) Antibiofouling polymer-coated superparamagnetic iron oxide nanoparticles as potential magnetic resonance contrast agents for *in-vivo* cancer imaging. *J Am Chem Soc*, **128**: 7383-9.
27. Kim JK, Kucharczyk W, Henkelman RM (1993) Cavernous hemangiomas: dipolar susceptibility artifacts at MR imaging. *Radiology*, **187**: 735-41.
28. Ahrens ET, Feili-Hariri M, Xu H, Genove G, Morel PA (2003) Receptor-mediated endocytosis of iron-oxide particles provides efficient labeling of dendritic cells for *in-vivo* MR imaging. *Magn Reson Med*, **49**: 1006-13.
29. Weissleder R (2002) Scaling down imaging: molecular mapping of cancer in mice. *Nat Rev Cancer*, **2**: 11-8.
30. Meyn RE, Milas L, Ang KK (2009) The role of apoptosis in radiation oncology. *Int J Radiat Biol*, **85**: 107-15.